Experimental Investigation and Modeling of Bubble Departure Frequency for Nucleate Pool Boiling Heat Transfer of Pure Liquids on Flat Heater

Samane Hamzekhani, Farhad Shahraki*, Davood Mohebbi-kalhori

Department of Chemical Engineering,
University of Sistan and Baluchestan, P.O. Box 98164-161, Zahedan, Iran
E-mail: s.hamzehkhani@pgs.usb.ac.ir, fshahraki@eng.usb.ac.ir,
davoodmk@eng.usb.ac.ir
*Corresponding author

Mohammad Reza Fardinpour

Department of Chemical Engineering,
Mahshahr Branch, Islamic Azad University, Mahshahr, Iran
E-mail: Fardinpour.mohamad@gmail.com

Abstract: In the present study, the response surface methodology is used to predict the bubble departure frequency of pure liquids using experimental data. Water, ethanol and methanol pure liquids were used as the testing fluid. The effects of vapor and liquid density difference, vapor and liquid viscosity, surface tension, thermal conductivity, heat flux on the vapor bubbles departure frequency on the heat transfer of boiling pool of pure liquids were investigated by response surface methodology. The results showed that the output of the Response surface methodology had a good overlap with the data of bubbles departure frequency of pure liquids. Also, the results for the bubble departure frequency show a good overlap between the models presented by the researchers and the experimental data and have good accuracy. In this research, a new model for the prediction of vapor bubble departure frequency, based on the Buckingham theory, in nucleate boiling is proposed, which predicts the experimental data with a satisfactory accuracy (9%).

Keywords: Bubbles Departure Frequency, Pool Boiling, Pure Liquid, Response Surface Methodology

Biographical notes: Samane Hamzekhani is currently a PhD candidate at Sisatan and Bluchestan University of Zahedan, Iran. He received his MSc in Chemical Engineering from Mahshar branch, IAU in 2014. **Farhad Shahraki** is currently a Professor at the Department of Chemical Engineering, Sistan and Baluchestan University. His current research interest includes simulation and Optimization. He received his PhD in Chemical Engineering from England University of Manchester in 2001. **Davood Mohebbi-kalhori** is currently an Assistant Professor at the Department of Chemical Engineering, Sistan snd Bluchestan University. He received his PhD in Chemical Engineering from Canada University of Sherbooke in 2008. **Mohammad Reza Fardinpour** received his MSc in Chemical Engineering from Mahshar Branch, IAU, Mahshar, Iran in 2013.

Research paper

1 INTRODUCTION

Evaporation at the solid-liquid phase interface is called boiling. The use of boiling phenomenon has been a topic that has been considered by researchers in this field for many years to increase the heat transfer coefficient and several studies have been conducted by researchers [1-10]. This process is one of the most widely used processes used in the industries such as oil, petrochemical, internal combustion engines and refrigerators due to its high heat transfer coefficient.

Bubble dynamics play a key role in the development of any analytical model for predicting heat transfer coefficient of pool boiling. Bubble dynamic parameters such as bubble departure frequency, bubble departure diameter and nucleation site density as well as the behavior of bubbles in the growth cycle and their departure from the surface are the basic mechanisms in modeling the boiling heat transfer process. One of the key and influential parameters on bubble dynamics is the frequency of bubble departure from the surface. The relations between f and D_b for an isolated bubble region in nucleate boiling are reported by Peebles and Garber [11], Cole [12] and others.

They [11] proposed the relation as:

$$f * D_b = 1.8 * \left(\frac{t_G}{t_G + t_W} \right) * \left(\frac{\delta g \Delta \rho}{\rho_L^2} \right)^{0.25} \quad (1)$$

Assuming the hydrodynamic region and the balance between drag and buoyancy forces, Cole [12] has proposed the following Equation.

$$f = {}_2\sqrt{\frac{4g(\rho_L - \rho_v)}{(3D_b \rho_L)}} \quad (2)$$

McFadden et al. [13] proposed the following Equation through dimensional analysis and available data.

$$fD_b^{0.5} = 17.5 \frac{cm^{0.5}}{s} \quad (3)$$

Zuber [14] has presented the following Equation by examining the available relationships and experimental data and according to the observations of Jacob et al.

$$D_b f = \frac{1.18}{2} \left[\frac{\delta g (\rho_{L-}\rho_v)}{\rho_L^2} \right]^{\frac{1}{4}} \quad (4)$$

Many correlations have been developed for the prediction of the bubble departure frequency for the nucleate pool boiling condition for different applications; the most important ones are summarized in "Table 1".

In this study, experiments related to the vapor bubble departure frequency on the flat surface for pool boiling of water, ethanol and methanol have been performed. Predicting bubble frequency from the proposed valid models requires calculation of parameters such as bubble diameter, bubble growth time and waiting time, which have their own complexities and limitations. The novelty of this paper is the use of response surface methodology to predict the bubble departure frequency based on heat flux and physical properties and the results of experiments performed in this study and data from the proposed models.

Table 1 Correlations suggested for the prediction of bubble departure frequency

Reference	Correlation
Peebles and Garber [11]	$f * D_b = 1.8 * \left(\frac{t_G}{t_G + t_W} \right) * \left(\frac{\delta g \Delta \rho}{\rho_L^2} \right)^{0.25}$
Cole [12]	$f = {}_2\sqrt{\frac{4g(\rho_L - \rho_v)}{(3D_b \rho_L)}}$
McFadden [13]	$fD_b^{0.5} = 17.5 \frac{cm^{0.5}}{s}$
Zuber [14]	$D_b f = \frac{1.18}{2} \left[\frac{\delta g (\rho_{L-}\rho_v)}{\rho_L^2} \right]^{\frac{1}{4}}$
Ivey [15]	(a) $\frac{f * D_b^{0.5}}{g^{0.5}} = 0.9$ (b) $\frac{f * D_b^{0.75}}{g^{0.5}} = 0.44(cm^{0.25})$
Stephen [16]	$f * D_b = \frac{1}{\pi} \left[\frac{g}{2} (D_b + \frac{4\delta}{\rho_L g D_b}) \right]^{0.5}$
Jacob and Fritz [17] Hamzekhani [18]	$f * D_b = 0.078$ $\frac{(f)_{solution}}{(f)_{water}} = 0.004(q)^{0.4527 - 0.4453x}$ $x \neq 0$

2 LABORATORY MACHINE AND TEST METHOD

2 .1. Heating Surface

Boiling tests were performed on flat surfaces made of stainless steel with a diameter of 20 mm and a length of 150 mm with a roughness of 0.09 μm by surface roughness tester model TR100/110.

2.2. Laboratory Machine

Figure 1 demonstrates the experimental setup of pool boiling used in this study with all the specifications. The main components of the device include: experiment container, main heater, auxiliary heater, power supply,

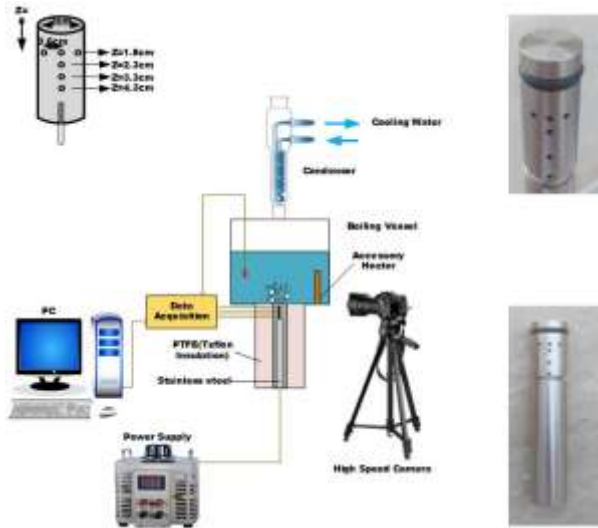and condenser and measuring equipment (temperature, pressure, ampere (current) and voltage).

Fig. 1   Scheme of pool boiling laboratory machine.

The test container is made of stainless steel 304, a cubic shape with inner dimensions of 20 cm * 15 cm * 20 cm. To observe the boiling process, a window with dimensions of 6 * 6/5 cm is embedded in the body of the container. All connections of the test container and windows have been leaked. The main stainless-steel heater is cylindrical and has 6 holes with a diameter of 1 mm to measure surface temperature. Type k thermocouples (with accuracy ±0.1k) were used to measure the surface temperature. To apply heat power to the heat transfer surface, a heater cartridge with 1cm diameter and 10cm length with power of 650 w is placed in the centre of the main heater. Cylindrical PTFE insulation with internal diameter of 20 mm and external diameter of 70 mm was utilized to prevent wasting heat. Two Viton O-Rings with diameter of 20 and 65 mm with a temperature of 300 ° C were used to leak the space between the test and the insulation container as well as the heater and insulation surface. To measure the liquid bulk temperature, two PT100 thermocouples are installed at two different locations and also to ensure the boiling fluid temperature, a thermocouple is installed on the upper part of the container (vapour phase). A condenser consisting of a spiral tube made of copper was used to condense the vapours. A barometer and a safety valve are installed to control the pressure in the body of the container. To adjust the voltage and reach the considered power at each stage of the experiment, a power supply of 300 watts made in Emersun was used. For imaging, a camera with a quality of 1200 frames per second with a shutter speed of 60 frames per second via a high magnification power is employed to calculate the bubble dynamic.

2.3. Experimental Method

Before each experiment, the test container is washed, dried, and leaked. Experiments were performed using deionized water under saturated conditions at 98 kPa. Experiments were repeated in two steps to make sure that precise outcomes have been obtained. After loading the tank with the experiment fluid, the auxiliary heater inside the chamber is switched on to bring the set to the saturation mode and after reaching the corresponding temperature, the main heater enters the circuit. Also, if needed to maintain fluid saturation, the auxiliary heater remains in the circuit especially at low fluxes (the input voltage to the auxiliary heater can be controlled). In this study, the criterion for maintaining saturation conditions is to compare the bulk temperature with the fluid saturation temperature at the experiment pressure. After reaching the saturated fluid condition, first the voltage of the power supply of heater is set to the highest voltage considered and after obtaining stable conditions, the relevant data is recorded. In this study, after reaching the stainless-steel cylinder temperature changes of 0.1 ° C and stability of these conditions for 3 minutes, the relevant data were recorded. To reach the next points of experiment, the heater voltage is reduced by step of 10 volts. This reduction has continued until the end of the bubble removal process. All the above steps for ethanol and methanol have been repeated after performing the tests for pure water, and all data were recorded and analysed.

3   CALCULATIONS AND ACCURACY

3.1. Calculation

Heat transfer coefficient of pool boiling can be calculated based on Newton's cooling Equation (Equation (11)).

$$h = \frac{q}{T_w - T_b} \tag{11}$$

In Equation (11), Tw is the surface temperature, Tb is the mass temperature and q is the heat flux applied to the liquid from the heater surface that from Equation (12) (assumption of linearity of distribution of temperature) and Equation (13) (Joule's the first law) can be calculated.

$$q = -k \left. \frac{dT}{dz} \right|_{surface} = -k \frac{T_i - T_1}{\Delta T axial} \tag{12}$$

$$q = \frac{V.I}{\pi.R^2} \tag{13}$$

In Equations (12) and (13), Z is the axial direction, I is the current intensity, V is the voltage and R is the radius of the heat transfer surface. According to the insulation around the heater by PTFE, it is assumed that the supposition of governing one-dimensional conductivity heat transfer mechanism in central direction is acceptable for this research. The analogy between the heat flux calculated from Equation (12) and (13) based on "Fig. 2" confirms this hypothesis and the absence of heat loss in radial direction.
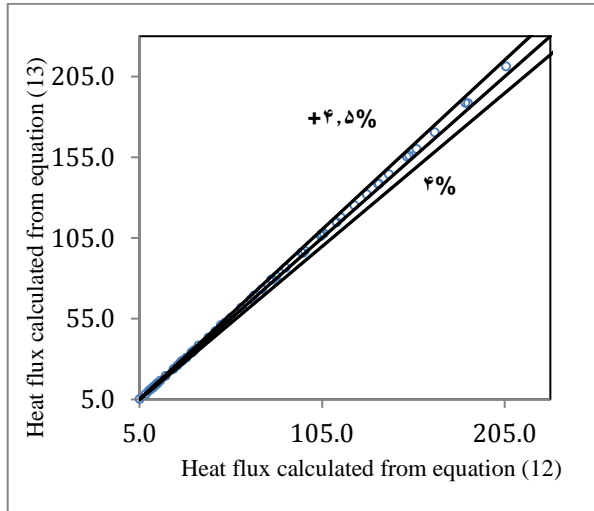

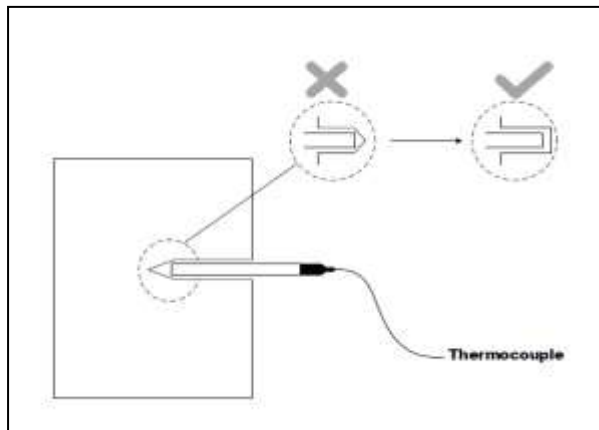**Fig. 2**   Heat flux dissipation analysis.

Fig. 3   How to create a thermocouple hole in the body of the main heater.

As it is shown in "Fig. 2", this difference is less than 4.5%. Two k-type thermocouples were installed at r = +0.5, r = -0.5 to measure the temperature distribution and ensure radial heat transfer. The results showed that the temperature at these two points is the same at each heat flux. Therefore, radial heat transfer can be neglected [19]. However, in this study, the heat loss rate has been considered for heat flux calculations. Also, based on the temperatures measured by the thermocouples, different

graphs were obtained at each heat flux with high accuracy (R = 0.99) ("Fig. 3"). The diagrams confirm linearity of distributing temperature in central direction (z). Therefore, for calculating T_w, Equation (15) can be used [20].

$$T = \alpha + \beta Z \qquad (14)$$

Since at $z = 0, T = T_w$
Thus, we have:

$$T_W = \alpha \qquad (15)$$

3.2. Accuracy
In this research, the following cases are considered in the design of the device and the experiment method to prevent error in the measurement of the parameters.
1- Using silicon paste with high thermal conductivity in the hole related to the thermocouples as well as between the main heater and the cartridge heater supplying heat power to remove the air layer and contact resistance
2-The flat end of the holes related the thermocouples in the main heater body using a lathe to remove the spatial layer ("Fig. 4").
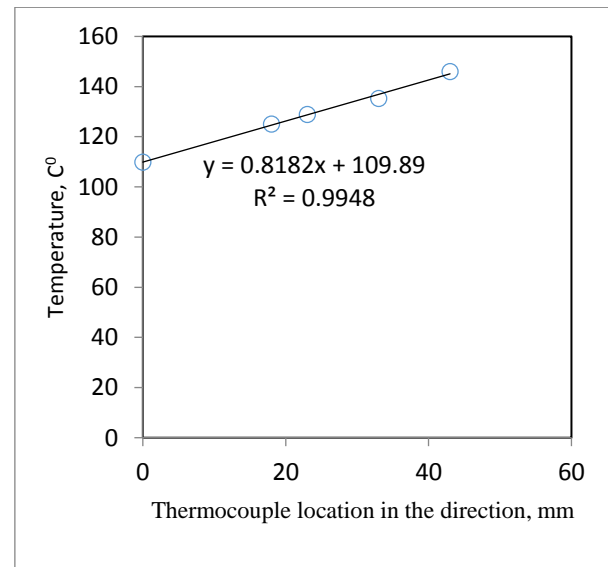

Fig. 4   Heater temperature changes in axial direction for 211 kW/m² heat flux and extraction of linear temperature relationship to determine surface temperature (for 211 KW/m² thermal fluid T_w = a = 109.89 in Equation 14).

3- Before each test step to remove air bubbles, the fluid heating process is performed at a point close to the saturation temperature.
4- The area around the test vessel is also completely insulated by fiberglass so that the temperature of the boiling fluid does not drop rapidly from saturation.

5- PTFE Teflon thermal insulation has been used to prevent heat loss of the original heater.

6- In this survey, Equation (16) is used to calculate the error of the calculated parameters.

$$v_p = \sqrt{\sum_{i=t}^{n} \left(\frac{\partial p}{\partial a_i} U a_i \right)^2} \qquad (16)$$

Where, P is the parameter considered, a is the measured parameter and U is the error related to the measured parameter. In this study, the maximum error measured for heat flux and heat transfer coefficient is 3.5% and 4.2%, respectively. "Table 2" shows the error values of the equipment used.

Table2 Error of calculated parameters and used equipment.

Parameter	Instrument	Uncertainty
Dimension	Coliseum	0.127%
Temperature	K-Tp	0.1K
Ampere	Keithley digital multi-meter	1%
Voltage	Keithley digital multi-meter	0.1V
Bulk temperature	Pt100	0.1K
Heat transfer surface area		0. 2538%
Heat flux		1.43-1.01%
Heat transfer coefficient		2.34-1.49%

4   RESULTS AND DISCUSSIONS

4.1. Validation of the Experimental Setup

In order to evaluate the accuracy of the laboratory device, the pure water data with the valid models provided by the researchers were evaluated. The results along with the heat transfer coefficient calculated from Gorenflo's [21], Alavi Fazel's [22], Stephan-Abdolsalam's [16] and Rohsenow's [23] have been shown in "Fig. 5".

Figure 5 shows a good overlap between the experimental data and the predicted values of the Equations with a mean absolute error of about 11% for Gorenflo's

correlation 13% for Alavi Fazel's correlation, 2% for Stephan-abdelsalam's correlation and 9% for Rohsenow's correlation.
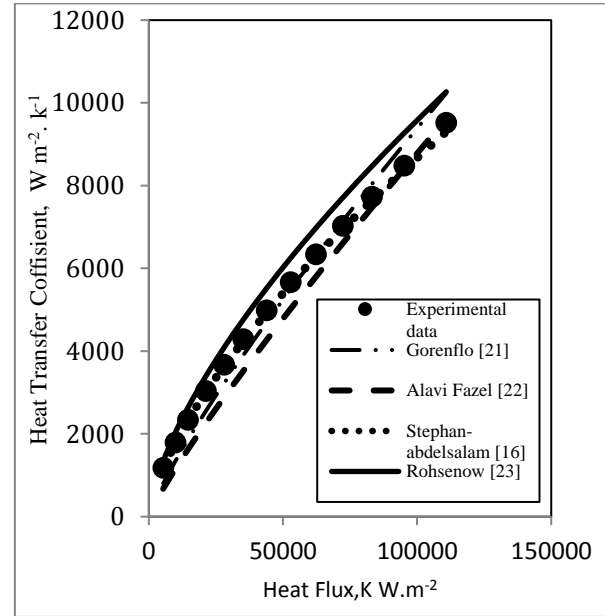

Fig. 5   Pool boiling setup validation. (Values of heat transfer coefficient with changes in heat flux).

5   BUBBLE DYNAMIC

After performing experiments and recording data and images related to the behavior of vapor bubbles in different heat fluxes for water, ethanol and methanol, the image data were analyzed by Edius software. At each heat flux, three 3-minute films have been recorded in stable conditions. The vapor bubble departure frequency is calculated for 10 to 30 nucleation sited and the average values obtained have been recorded as the bubble departure frequency for the test fluid at the corresponding heat flux. Figure 6 shows the bubble frequency changes for water, ethanol, and methanol with heat flux. As shown in "Fig. 6", the frequency of vapor bubbles has increased with increasing heat flux. Reducing the waiting time of bubbles and increasing the growth rate of vapor bubbles and reducing the growth time of bubbles by increasing the heat flux are the causes of this phenomenon (Equation (17)).

$$f = \frac{1}{t_w + t_G} \qquad (17)$$

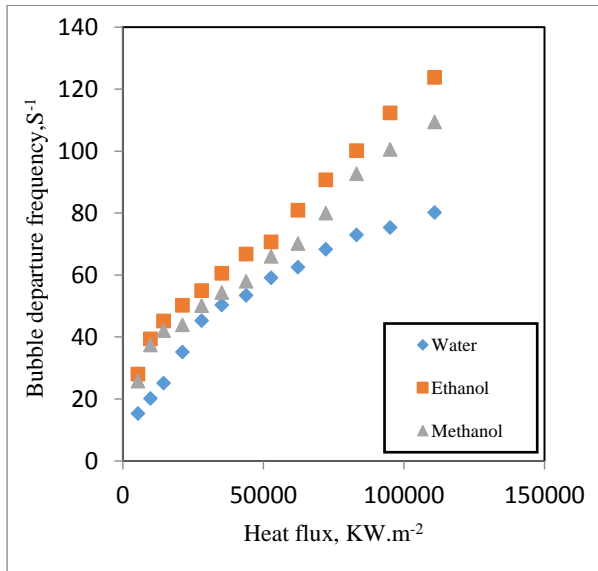Where, t_w and t_G are waiting time and growth time, respectively.

Fig. 6   Bubble departure frequency water, ethanol and methanol at various heat fluxes.

In studies conducted by [12-16], [18], the proposed relationships for bubble frequency include the diameter of the vapor bubbles. In most of the proposed Equations, the bubble frequency calculation Equation has been proposed as the product of the bubble diameter multiplied by the bubble frequency with a certain power. These results show a close and inverse correlation between these two parameters. In this research, the Zuber Equation has been used to calculate the bubble diameter Zuber [14]. Figure 7 shows the bubble diameter changes with increasing heat flux for water, ethanol and methanol.
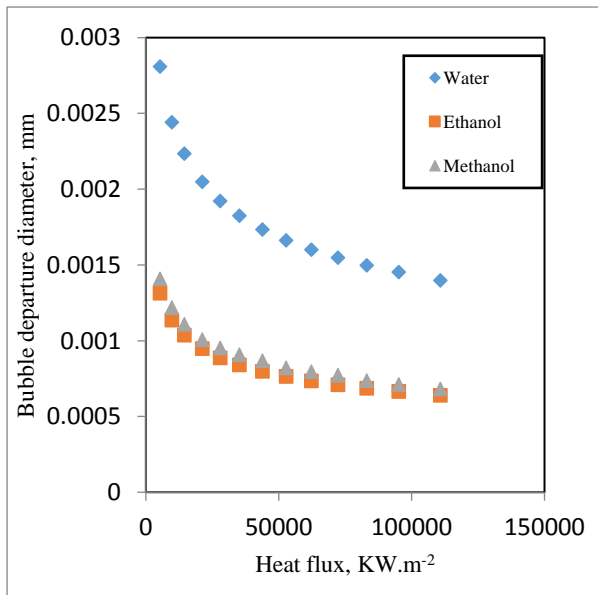

Fig. 7   Bubble departure diameter of water, ethanol and methanol at various heat fluxes.

According to Figure 7, the diameter of the vapor bubbles decreases for all three fluids tested with increasing heat flux. Also, water has the highest and ethanol the lowest bubble diameters. In confirmation of this result and the inverse relationship between diameter and frequency of vapor bubbles as shown in "Fig. 6", water has the highest and ethanol the lowest values of the bubble frequency. Figure 8 clearly shows this relationship.
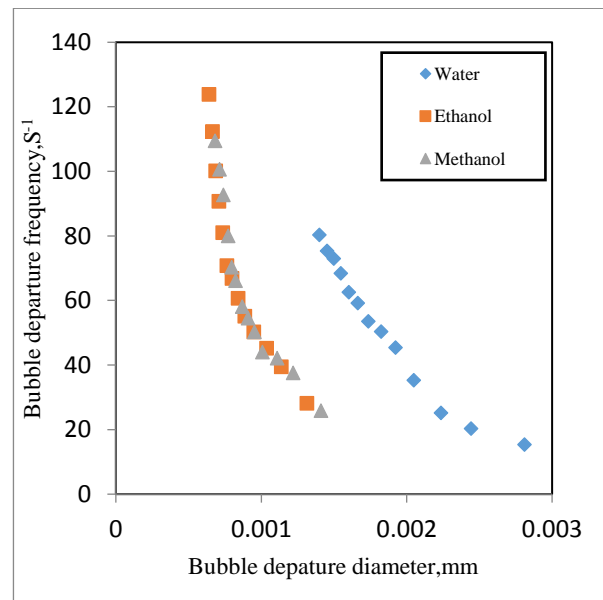

Fig. 8   Measured bubble departure frequency of (water, ethanol and methanol) compared with Bubble departure diameter model Zuber [14].

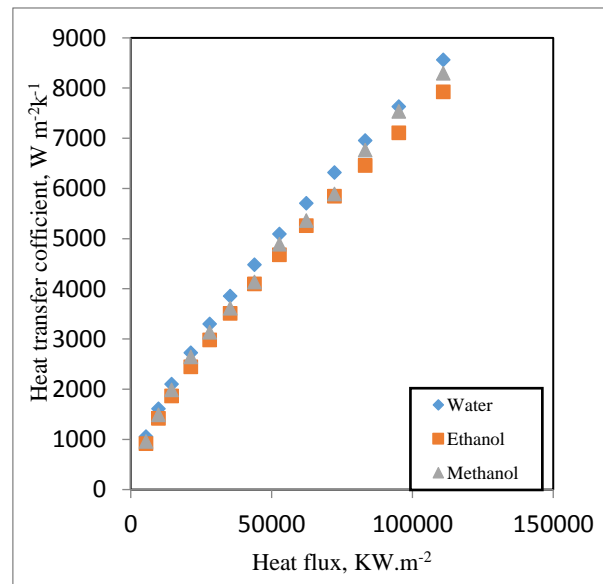Figure 9 shows the changes in heat transfer coefficient with heat flux for water, ethanol and methanol.

Fig. 9   Heat transfer coefficient of water, ethanol and methanol at various heat fluxes.

The results show that the highest heat transfer coefficient is associated with water and the lowest has been obtained for ethanol. From the perspective of vapor bubble dynamics and based on "Figs. (6-9)", ethanol with the highest bubble frequency and lowest bubble diameter values has had the lowest heat transfer coefficient and, water with the highest bubble diameter values and the lowest bubble frequency values has the highest heat transfer coefficient. Based on this, it can be concluded that the effect of bubble diameter over the bubble frequency on the heat transfer coefficient is dominant. Figures (10-12) shows a comparison between the laboratory data and the proposed relationships for the bubble frequency. In this study, the Zuber Equation has been used to calculate the bubble diameter.
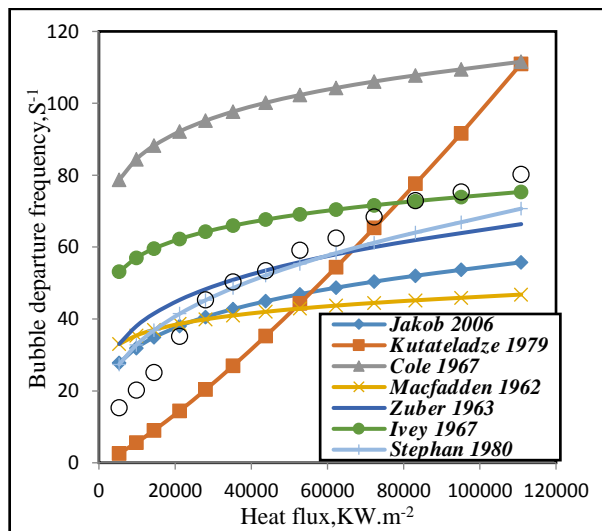

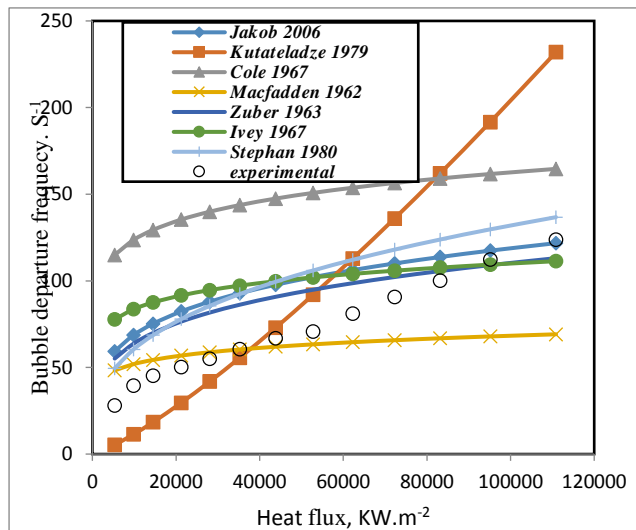**Fig. 10**   Comparison of experimental data of water bubble departure frequency with experimental relationships.

Fig. 11   Comparison of experimental data of ethanol bubble departure frequency with experimental relationships.
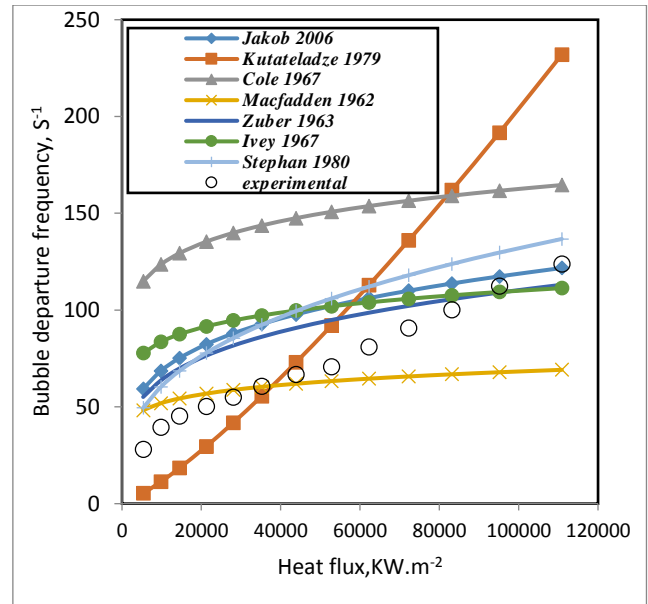

Fig. 12   Comparison of experimental data of methanol bubble departure frequency with experimental relationships.

"Table 3" shows the mean error between the experimental data and the presented relationships.

Table 3 The mean error between the experimental data and the presented relationships

Average percentage error	Jakob 2006 [18]	Kutate ladze 1979 [24]	Cole 1967 [12]	Zuber 1963 [14]	Ivey 1967 [15]	Stephan 1980 [16]
Water	28.8	70.8	50.1	19.5	27.2	15.2
Ethanol	28.2	88.4	52.2	24.4	31.5	28.9
Methanol	30.1	77.4	55.4	26.1	34.3	30.7

As shown in Table 3, there is a good overlap between the experimental data and the relationships presented. Peebles, Mikic and Rohsenow, models have not been studied due to the need for growth time, waiting time and lack of access to this data of Peebles and Garber [11], Mikic and Rohsenow [23].

6   EXPERIMENTAL DESIGNS

5.1. Response Surface Methodology
In Response Surface Methodology (RSM), a model with the form of "Eq. (18)" is fitted to experimental data and, by optimization methods, the best coefficients for the model are calculated.

$$Y = \beta_0 + \sum_{i=1}^{k} \beta_i x_i + \sum \sum_{i \prec j} \beta_{ij} x_i x_j + \sum_{i=1}^{k} \beta_{ij} x_i^2 + \varepsilon \quad (18)$$

Where, K is the number of factors, x_i are linear terms (input variables), x_i^2 are quadratic terms, and $x_i x_j$ are interaction terms, Y is the corresponding response (experimental data).

β_0, β_i, β_{ij} and β_{ii} are the coefficients of the model. The adequacy of the model and significance of the coefficients should be analyzed by statistical methods. An analysis of variance (ANOVA), F-value, P-value of the model, R^2-adjusted and R^2 statistic was performed to evaluate significant differences between factors and to validate the model and check the adequacy of the developed model [25-26]. Central composite design (CCD) is one of the most popular RSM techniques. In the present study, the experiments were designed by the CCD technique. This technique was used to investigate the effect five parameters of pool boiling system for bubble departure frequency as the response. Vapor-liquid density difference, vapor-liquid viscosity, surface tension, thermal conductivity, heat flux were chosen as the parameters and bubble departure frequency was chosen as the response.

7   RESULT AND DISCUSSIONS

In this study, three pool boiling systems for modeling and optimization of bubble departure frequency were considered. The effects of five main parameters on the bubble departure frequency were performed based on the Central Composite Design (CCD). Low and high values of the pool boiling systems designed variables, which are used for experimental design, can be seen in "Table 4". Data obtained from simulations were investigated for the response of three systems, using the

models named linear, two-factor interaction (2FI), quadratic and cubic.

Table 4 Low and high values of the pool boiling systems designed variables

Material	Factor	Unit	Coded factor level	
			-1	1
Water				
	q	W/m^2	110862	5335.32
	k	W/m.s	0.6710	0.6697
	pl-pv	Kg/m^3	958.85	954.83
	μl-μv	Pa.s	12.765	11.0419
	$\square$	N/m	0.0580	0.0566
Methanol				
	q	W/m^2	5335.3	110862
	k	W/m.s	0.1861	0.18769
	pl-pv	Kg/m^3	737.21	743.864
	μl-μv	Pa.s	33.362	37.8457
	$\square$	N/m	0.0176	0.01845
Ethanol				
	q	W/m^2	5335.3	110862
	k	W/m.s	0.1548	0.1569
	pl-pv	Kg/m^3	723.30	730.062
	μl-μv	Pa.s	33.362	37.8457
	$\square$	N/m	0.0164	0.01703

"Table 5" shows the results for each of the process conditions suggested by the RSM design for pool boiling system. Furthermore, considering the values of standard deviation, higher R^2, adjusted R^2 and predicted R^2 of the two-factor interaction (2FI), model was found for bubble departure frequency. The model summary statistics and the results of ANOVA analysis for selecting the model of bubble departure frequency for three systems are shown in "Table 6". "Table 7" gives an insight into the linear, interaction and quadratic effects of the factors for the responses investigated. According to the experimental results for water, methanol and ethanol pool boiling system which are reported in "Table 4", and Equation 18, the response surface models with actual variables have been written responses as:

Table 5 RSM results for three pool boiling system

Material	Run	q	k	pl-pv	μl-μv	$\square$	f
Water		W/m^2	W/m.s	Kg/m^3	Pa.s	N/m	1/S
	1	5335.32	0.66978832	958.8	12.7	0.05808	15.324
	2	9837.59	0.66997	958.2	12.5	0.05789	20.2332
	3	14508.9	0.67011	957.8	12.3	0.0577	25.158
	4	21229.7	0.67025	957.4	12.1	0.0575	35.21
	5	28035.9	0.67037	957.0	11.9	0.05746	45.3256
	6	35229.7	0.670488	956.6	11.8	0.05734	50.3698
	7	43836.5	0.67058	956.3	11.6	0.05723	53.485
	8	52795.5	0.67067	956.0	11.5	0.05713	59.125
	9	62249.7	0.67074	955.8	11.4	0.05705	62.564
	10	72259.09	0.67083	955.5	11.3	0.0569	68.398
	11	83139.5	0.67090	955.3	11.2	0.0568	72.956
	12	95135.3	0.67097	955.0	11.1	0.05678	75.3
	13	110861.9	0.671047	954.8	11.0	0.05669	80.265

Methanol							
	1	5335.32	0.18769	743.8	22.9	0.01845	25.825
	2	9837.59	0.18747	742.9	21.6	0.01814	37.5055
	3	14508.9	0.18732	742.2	20.7	0.01809	42.1125
	4	21229.7	0.18717	741.6	19.9	0.01803	44.004
	5	28035.9	0.18698	740.8	18.8	0.01795	50.2
	6	35229.7	0.18681	740.0	17.9	0.01789	54.455
	7	43836.5	0.18664	739.3	17.0	0.01782	58.0635
	8	52795.5	0.18660	739.1	16.7	0.01780	66.095
	9	62249.7	0.18643	738.4	15.9	0.01774	70.2455
	10	72259.09	0.18629	737.8	15.2	0.01769	80.0213
	11	83139.5	0.18629	737.8	15.2	0.01769	92.7
	12	95135.3	0.18622	737.5	14.8	0.01766	100.6
	13	110861.9	0.1861	737.2	14.5	0.017	109.43
Ethanol							
	1	5335.3	0.67104	730.0	37.8	0.01703	28.115
	2	9837.5	0.15697	729.6	37.5	0.01699	39.4275
	3	14508.9	0.15685	729.1	37.1	0.01694	45.1675
	4	21229.7	0.15668	728.2	36.6	0.01687	50.275
	5	28035.9	0.15642	728.1	36.5	0.01686	55.06
	6	35229.7	0.15639	727.0	35.7	0.01676	60.6025
	7	43836.5	0.15603	726.1	35.1	0.01667	66.81
	8	52795.5	0.15575	725.3	34.6	0.01660	70.725
	9	62249.7	0.15549	725.0	34.4	0.01657	80.9978
	10	72259.0	0.1554	724.7	34.3	0.01655	90.74
	11	83139.5	0.15532	724.1	33.9	0.01649	100.147
	12	95135.3	0.15513	723.7	33.6	0.01645	112.325
	13	110861.9	0.15498	723.3	33.3	0.01641	123.81

Table 6 Model summary statistics and analysis of variance (ANOVA) of the RSM model corresponding to the response: performance

Material		Sum of Squares	df	Mean Square	F Value	p-value Prob > F
Water						
	Model	5596.32	5	1119.26	580.30	< 0.0001
	Linear	R^2=0.9976	R^2adj=0.9959	R^2 pre=0.9921		Suggested
Methanol						
	Model	7850.49	5	1570.10	338.35	< 0.0001
	Linear	R^2=0.995	R^2adj =0.992	R^2 pre=0.9913		Suggested
Ethanol						
	Model	10130.92	5	2026.18	814.76	< 0.0001
	Linear	R^2=0.9971	R^2adj =0.995	R^2 pre=0.991		Suggested

Table 7 ANOVA results for the terms of the second-order polynomial Equations for ethanol, methanol, water

Material		Sum of Squares	df	Mean Square	F Value	p-value Prob > F
Water						
	A-q	1.29	1	1.29	0.6709	0.4397
	B-☐	13.05	1	13.05	6.77	0.0354
	C-k	12.92	1	12.92	6.70	0.036
	D-pl-pv	13.05	1	13.05	6.76	0.0354
	E-μl-μv	13	1	13	6.74	0.0356
Methanol						
	A-q	92.36	1	92.36	19.90	0.0029
	B-☐	7.33	1	7.33	1.58	0.2490
	C-k	0.4712	1	0.4712	0.1015	0.7593
	D-pl-pv	0.4795	1	0.4795	0.1033	0.7573
	E-μl-μv	0.4023	1	0.4023	0.0867	0.7770

Ethanol						
	A-q	54.02	1	54.02	21.72	0.0023
	B-□	15.49	1	15.49	6.23	0.0412
	C-k	15.53	1	15.53	6.24	0.0411
	D-pl-pv	15.15	1	15.15	6.09	0.0429
	E-μl-μv	15.64	1	15.64	6.29	0.0405

Equation (19) obtained for water shows that surface tension, thermal conductivity, liquid-vapor viscosity difference and heat flux in a linear manner with a negative constant slope have the highest effect on bubble departure frequency, and liquid-vapor density difference affects the bubble departure frequency linearly with positive slope.

$$f = -3.71336E + 08 - 0.00057 * q - 1.39351E + 09 * \sigma - 2.48563E + 08 * k + 6.533069E + 05 * \rho_l - \rho_v - 5.82733E + 05 * \mu_l - \mu_v \qquad (19)$$

The Equation obtained for methanol shows that the liquid-vapor density difference and heat flux in a linear manner and with a negative constant slope have the maximum effect on bubble departure frequency, where the effect of density is greater than the heat flux. The remaining three parameters linearly and with a negative coefficient affect the bubble departure frequency, which respectively, the thermal conductivity, surface tension and the liquid-vapor viscosity difference have the greatest decrease on the bubble frequency.

$$f = +1.04321E + 05 + 0.000824 * q - 38801.86 * \sigma - 4.81617E + 06 * K + 1074.95762 * \rho_l - \rho_v - 32.47335 * \mu_l - \mu_v \qquad (20)$$

The Equation obtained for ethanol shows that surface tension and heat flux affect linearly and with the highest positive slope, and thermal conductivity, the liquid-vapor viscosity difference and the liquid-vapor density difference have the greatest negative effect on the bubble departure frequency in linear form, respectively. Also, no interaction effect, quadratic effect and cubic effect between parameters on response f were detected.

$$f = +3.47767E + 08 + 0.000933 * q + 1.29096E + 10 * \sigma - 2.87797E + 09 * k - 1.4939E + 05 * \rho_l - \rho_v - 1.80158E + 05 * \mu_l - \mu_v \qquad (21)$$

The values of the responses determined using the regression Equations were compared with the obtained experimental data, and the results are presented in "Fig. 13". As can be seen, the model shows the good prediction of the experimental data. Therefore, based on the statistical tests and data comparison the models can be considered adequate for water, ethanol, methanol pool boiling system simulations and optimization.
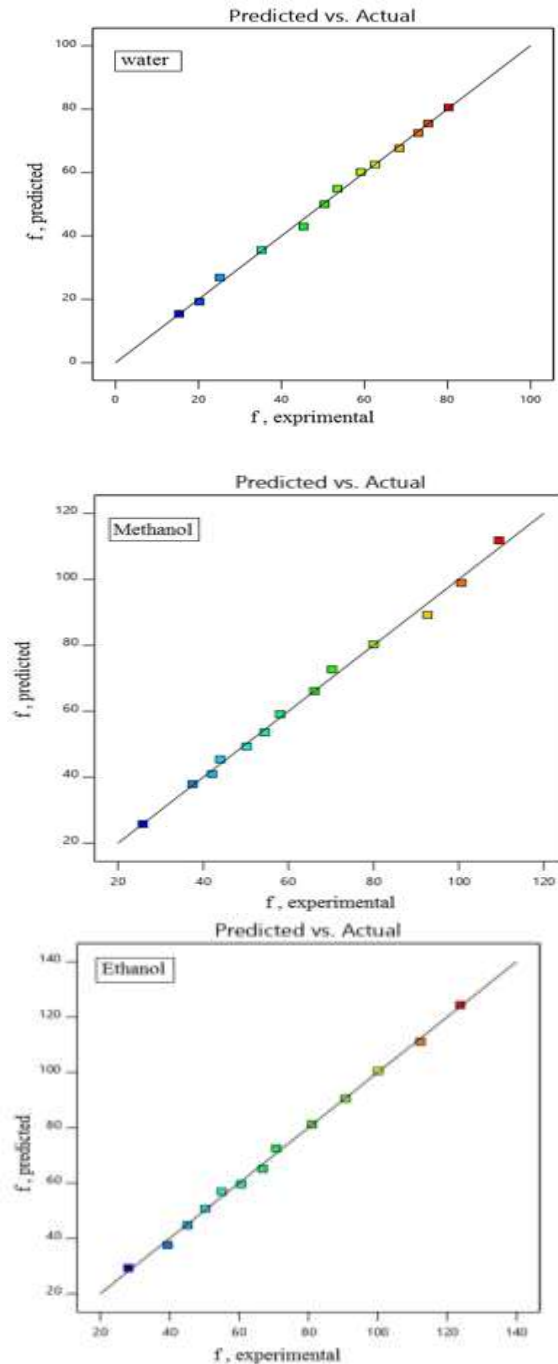

Fig. 13 Comparison between the experimental and the predicted water, methanol and ethanol pool boiling process performance index (f) determined by the RSM model.

As it can be seen in "Tables 5 and 6", P-value is smaller than 0.0001, the F-values are so high, and the coefficient of multiple determinations (R^2) and the adjusted statistic coefficient (R^2_{adj}) are in agreement for the response. According to this tables, it can be deduced that the linear model was significant and adequate to represent the actual relationship between the response (f) and five variables (vapor-liquid density difference, vapor-liquid viscosity, surface tension, thermal conductivity, heat flux) for three pool boiling systems.

8   NEW MODEL

In this study, based on dimensional analysis, a quasi-experimental model has been proposed to calculate the bubbles departure frequency. Parameters such as bubbles departure frequency, vapor-liquid density difference, vapor density, heat flux, surface tension, liquid viscosity, vapor viscosity, liquid thermal conductivity, vapor thermal conductivity, ratio of fluid contact angle to water contact angle can be effective as 10 effective parameters with four MLTθ dimensions. According to π Buckingham's theory, dimensionless groups are obtained as follows:

$$\pi_1 = \frac{\rho_v}{\Delta\rho} \tag{22}$$

$$\pi_2 = \frac{q}{\delta f} \tag{23}$$

$$\pi_3 = \frac{\mu_L}{\mu_v} \tag{24}$$

$$\pi_4 = \frac{k_v}{k_l} \tag{25}$$

$$\pi 5 = \frac{\theta_{fluid}}{\theta_{water}} \tag{26}$$

Based on dimensionless groups (22) to (26), relationship (27) is established.

$$\frac{q}{\delta f} = f\left((\frac{\rho_v}{\Delta\rho}),(\frac{\mu_L}{\mu_v}),(\frac{k_v}{k_l}),(\frac{\theta_{fluid}}{\theta_{water}})\right) \tag{27}$$

According to relationship (27), there is:

$$f = C_0(\frac{\rho_v}{\Delta\rho})^{c_1}(\frac{\mu_L}{\mu_v})^{c_2}(\frac{k_v}{k_l})^{c_3}(\frac{\theta_{fluid}}{\theta_{water}})^{c_4}(\frac{q}{\delta})^{c_5} \tag{28}$$

In this research, using the MATLAB program and the data of the bubble frequency, the coefficients C_0 to C_5 have been calculated and the proposed model has been presented as Equation (29).

$$f = 0.4(\frac{\rho_v}{\Delta\rho})^{0.0625}(\frac{\mu_L}{\mu_v})^{0.035}(\frac{k_v}{k_l})^{0.1}(\frac{\theta_{fluid}}{\theta_{water}})^{1.0625}(\frac{q}{\delta})^{0.5} \tag{29}$$

Figure 14 shows a comparison between the experimental data and the proposed model. The error rate calculated based on Equation (27) is less than 9% (water 4%, ethanol 7%, methanol 1%).
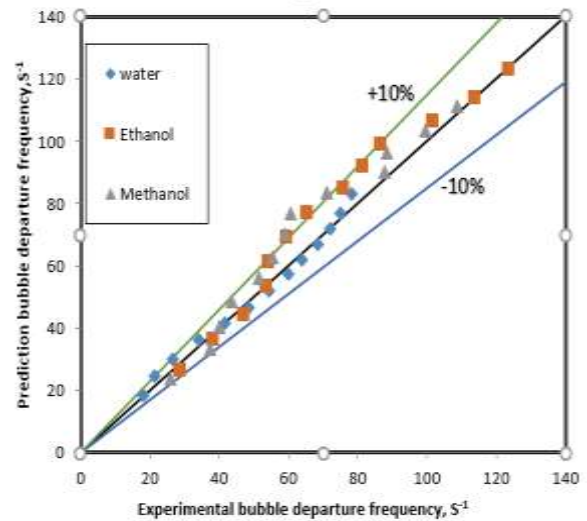

Fig. 14   Experimental data versus predicted of bubble departure frequency by the new model.

9   CONCLUSIONS

In this study, the bubble departure frequency on a flat surface for boiling pool water, ethanol and methanol using a response surface methodology has been discussed and the following results have been obtained.

1- Based on the data obtained for heat transfer coefficient, the experimental data showed the best overlap with the models proposed by Stephan-abdelsalam (error 2%) and Rohsenow (error 9%).

2- The results show an increase in the bubble frequency with an increase in heat flux. Reducing the growth time and waiting time of the bubble by increasing the heat flux is the cause of this phenomenon. Water and ethanol have the lowest and highest bubble frequencies, respectively.

3- The Bubble diameter decreases with increasing the heat flux. Water and ethanol have the highest and lowest bubble diameters, respectively.

4- According to the results, with decreasing bubble diameter, the bubbles departure frequency increased. Other proposed models have confirmed such a result.

5- The results for the bubble departure frequency show a good overlap between the experimental models and the laboratory data.

6- The data obtained for the bubble departure frequency show a good overlap between the experimental results and the predicted results of the RSM.

7- In this research, a quasi-experimental model has been presented based on the data of the bubble departure frequency and using dimensional analysis and MATLAB program for the bubbles departure frequency of pure liquids (water, ethanol and methanol). The error of the model with experimental results has been less than 9%.

10   APPENDIX OR NOMENCLATURE

D	Diameter (m)	p	Density ($kg\ m^{-3}$)
f	Bubble departure frequency (s^{-1})	□	Surface tension ($N\ m^{-1}$)
g	Gravity ($m\ s^{-2}$)	Δ	Difference
h	Heat transfer coefficient ($W\ m^{-2}\ K^{-1}$)	μ	Dynamic viscosity (Pa s)
I	Electrical current (A)		
K	Thermal conductivity ($W\ m^{-1}K^{-1}$)	Subscripts	
q	Heat flux ($W\ m^{-2}$)	b	Bubble
t	Time (s)	l	Liquid
T	Temperature (K)	v	Vapor
V	Velocity ($m\ s^{-1}$) or Voltage (V)	G	Growth
		W	Waiting

ACKNOWLEDGMENTS

REFERENCES

[1] Vasei Moghadam, A., Goshayeshi, H. R., Experimental Investigation of Pool Boiling of Single Wall Carbon Nanotubes (SWCNTs) with Different Grooved Surfaces, Int J Advanced Design and Manufacturing Technology, Vol. 12, 2019, pp. 77-84.

[2] Gajghate, S. S., Barathula, S., Das, S., Saha, B. B., and Bhaumik, S., Experimental Investigation and Optimization of Pool Boiling Heat Transfer Enhancement Over Graphene-Coated Copper Surface, J. Therm. Anal. Calorim, Vol. 140, 2020, pp. 1393–1411.

[3] Hamzekhani, S., Maniavi Falahieh, M., Kamalizadeh, M. R., and Salmaninejad, M., Bubble Dynamics for Nucleate Pool Boiling of Water, Ethanol and Methanol Pure Liquids under the Atmospheric Pressure, Journal of Applied Fluid Mechanics, Vol. 8, 2015, pp. 893-898.

[4] Khooshehchin, M., Mohammadidoust, A., and Ghotbinasab, S., An Optimization Study on Heat Transfer of Pool Boiling Exposed Ultrasonic Waves and Particles Addition, International Communications in Heat and Mass Transfer, Vol. 114, 2020, pp. 104558.

[5] Sarafraz, M. M., Experimental Investigation on Pool Boiling Heat Transfer to Formic Acid, Propanol And 2-Butanol Pure Liquids the Atmospheric Pressure, Journal of Applied Fluid Mechanics, Vol. 6, 2013, pp. 73-79.

[6] Sitter, J. S., Snyder, T. J., Chung, T. N., and Marslon, P. L., Terrestrial and Microgravity Pool Boiling Heat Transfer from A Wire in An Acoustic Field, Int. J. Heat Transfer, Vol. 41, 1998, pp. 2143-2155.

[7] Hamzekani, S., Maniav Falahieh, M., and Akhbari, A., Bubble Departure Diameter in Nucleate Pool Boiling at Saturation: Pure Liquids and Binary Mixtures, Int. J. Refrigeration, Vol. 46, 2014, pp. 50-58

[8] Gupta, S. K, Misra, R. D., Experimental Study of Pool Boiling Heat Transfer on Copper Surfaces with Cu-Al2O3 Nanocomposite Coatings, International Communications in Heat and Mass Transfer, Vol. 97, 2018, pp. 47-55.

[9] Choi, G., Shim, D. I., Lee, D., Kim. B. S., and Cho, H. H., Enhanced Nucleate Boiling Using a Reduced Graphene Oxide-Coated Micropillar, International Communications in Heat and Mass Transfer, Vol. 109, 2019, pp.104331.

[10] Alavi Fazel, S. A., A Genetic Algorithm-Based Optimization Model for Pool Boiling Heat Transfer on Horizontal Rod Heaters at Isolated Bubble Regime, Heat Mass Transfer, Vol. 53, 2017, pp. 2731-2744

[11] Peebles, F. N., Garber, H. J., Studies on Motion of Gas Bubbles in Liquids, Chem. Eng. Prog, Vol. 49, 1953, pp. 88–97.

[12] Cole. R., Bubble Frequencies and Departure Volumes at Sub Atmospheric Pressures, AICHE J, Vol. 13, 1967, pp. 779-783

[13] McFadden, P. W., Grassman, P., The Relation Between Bubble Frequency and Diameter During Nucleation Pool Boiling, International Journal Heat Mass Transfer, Vol. 5, 1962, pp.169-173

[14] Zuber, N., Nucleate Boiling the Region of Isolated Bubbles Similarity with Natural Convection, Int. J. Heat Mass Transfer, Vol. 6, 1963, pp. 53–65.

[15] Ivey, H., Relationships Between Bubble Frequency Departure Diameter and Rise Velocity in Nucleate Boiling, International Journal Heat and Mass Transfer, Vol. 10,1967, pp 1023-1040.

[16] Stephan, K., Abdelsalam, K., Heat Transfer Correlation for Natural Convection Boiling, International Journal of Heat and Mass Transfer, Vol. 23, 1980, pp. 73-87.

[17] Chen, Y., Groll, M., Mertz, R., and Kulenovic, R., Bubble Dynamics of Boiling of Propane and Iso-Butane on Smooth and Enhanced Tubes, Experimental Thermal and Fluid Science, Vol. 28, 2004, pp. 171–178.

[18] Kim, J., Kim, M. H., On the Departure Behaviors of Bubble at Nucleate Pool Boiling, International Journal of Multiphase Flow, Vol. 32, 2006, pp. 1269–1286.

[19] Hamzekhani, S., Maniavi Falahieh, M., Kamalizadeh, M. R., and Salmaninejad, M., Bubble Dynamics for Nucleate Pool Boiling of Water, Ethanol and Methanol Pure Liquids under the Atmospheric Pressure, Journal of Applied Fluid Mechanics, Vol. 8, 2015, pp. 893-898.

[20] Sarafraz, M. M., Hormozi, F., Experimental Investigation on The Pool Boiling Heat Transfer to Aqueous Multi-Walled Carbon Nanotube Nanofluids on The Micro-Finned Surfaces, International Journal of Thermal Sciences, Vol. 100, 2016, pp. 255-266.

[21] Gorenflo, D., Pool Boiling. In: VDI Heat Atlas (chapter Ha), 1993.

[22] Alavi fazel, S. A., Roumana, S., Bubble Dynamics for Nucleate Pool Boiling of Electrolyte Solutions, J. Heat Transfer, Vol. 132, 2010, pp. 1-7.

[23] Mikic, B. B., Rohsenow, W. M., Bubble Growth Rates in Non-Uniform Temperature Field, progress in Heat and Mass Transfer, Vol. 2, 1969, pp. 283-293.

[24] Kutatelaze, S. S., Gognim, I. I., Growth Rate and Detachment Dimeter of a Vapor Bubble in Free Convection Boiling of a Saturated Liquid, High Temp, Vol. 17, 1979, pp. 667-671.

[25] Hamzekhani, S., Sardashti Birjandi, M. R., and Shahraki, F., Modeling and Optimization of the Bubble Detachment Diameter for a Pool Boiling System, Chem. Eng, Technol, Vol. 45, 2022, pp. 1–13.

[26] Muthuvelayudham, R., Viruthagir, T., Application of Central Composite Design Based Response Surface Methodology Inparameter Optimization And On Cellulase Production Using agricultural Waste, International Journal of Agricultural and Biosystems Engineering, Vol. 4, 2010, pp. 12-19.